

## Supplementary Discussion

### D1 Endemics-area relationship (EAR) and its relation to the SAR

The EAR comprises the relationship between study area and the number of species that are endemic (i.e. globally restricted) to it. In contrast to the SAR, it can be used for estimation of species losses after a given area is destroyed<sup>9</sup>, because all endemic species which go eventually extinct in this area are by definition also globally extinct. However, a connection with the SAR exists, as an increase of the EAR at small scales corresponds to the decrease of the total number of species with decreasing area at large scales. Here we further develop this link.

The EAR addresses the number of species  $S_E$ , endemic to area  $A_E$  (Supplementary Fig. 1). Endemic species by definition do not occur outside the area  $A_E$ , i.e. in the remaining area  $A_R$  ( $A_R = A_{TOT} - A_E$ , where  $A_{TOT}$  is the area of the whole studied region). The total number of species which do occur in  $A_R$  is thus  $S_R = S_{TOT} - S_E$ , where  $S_{TOT}$  is the known number of all species occurring in the whole study region,  $A_{TOT}$ .

Let us now consider the SAR relating  $S_R$  to  $A_R$ , and assume that species richness  $S_R$  increases with  $A_R$  according to the power-law. Note that although the power-law cannot represent an appropriate description of the SAR across all spatial scales<sup>13,14</sup>, it is a good approximation for a limited range of spatial scales<sup>1</sup>. For such a limited range of spatial scales we can thus contend that

$$S_R = cA_R^z = c(A_{TOT} - A_E)^z. \quad (\text{Eq. S1})$$

Therefore

$$S_E = S_{TOT} - S_R = S_{TOT} - c(A_{TOT} - A_E)^z \quad (\text{Eq. S2})$$

(Supplementary Fig. 2). This function is apparently more complex than a simple power function and its behaviour in logarithmic space is not a simple straight line. However, its behaviour may simplify under particular conditions. Namely, if the slope  $z$  of the species-area relationship for  $S_R$  approaches 1, as indeed is the case of the SAR at very large spatial scales (see the main text), the above equation simplifies as

$$S_E \approx S_{TOT} - c(A_{TOT} - A_E) = S_{TOT} - cA_{TOT} + cA_E \quad (\text{Eq. S3})$$

And since  $c$ ,  $S_{TOT}$ , and  $A_{TOT}$  are constants,  $S_E$  is a simple linear function of  $A_E$  in such a case. Moreover, if  $z$  approaches 1,  $S_{TOT} \sim cA_{TOT}$ , and the resulting function is then linear also in a log-log space, with slope  $z \approx 1$  (Supplementary Fig. 2). Additionally, if the slope  $z$  of the SAR is lower than 1, the slope of the EAR should be higher than 1, which is in agreement with our observations (see the main text). The reason is that the SAR with  $z < 1$  is downward-decelerating (concave), and this corresponds to upward-accelerating (convex) EAR, for which  $z > 1$  (red line in Supplementary Fig. 2).

This reasoning relies on significant simplifications. Most importantly, it assumes that the effect of increase of  $A_E$  is symmetric with the effect of the decrease of  $A_R$ , and vice versa. In nature the shapes of these areas are expected to be different<sup>16</sup> (see Supplementary Fig. 1) with consequences for the expected SAR and EAR shapes and slopes. The shape of the area certainly plays a role for the overall SAR shape<sup>33</sup>, and the variation of the shape of  $A_R$  probably affects the deviations observed in our data. Further, our considerations for the SAR concerning the relationship between  $A_R$  and  $S_R$  apply to contiguous areas, a condition which may not hold, especially if the  $A_E$  is large. However, even in just approximate form the above considerations are able to advance the qualitative understanding of the relationships between the EAR and the SAR. The development of a full quantitative theory for EAR–SAR association is beyond the scope of our study.

## D2 Theoretical underpinning of the continental SAR and EAR: expected shape

Several theoretical approaches have predicted the upward-accelerating SAR at large spatial scales<sup>2–6</sup>. Although they have been based on various foundations and different explanatory frameworks, ranging from simple geometric models<sup>2,29</sup> to neutral dynamics<sup>4,5</sup>, the fundamental arguments are highly similar. As the sampling area increases in size beyond that of most species' ranges, more and more ranges are comprised within just one or a few sampling windows, i.e. each species occurs just in one "site". The case in which every species occupies just one site is characterized by the SAR whose slope approaches 1; the number of species is thus getting proportional to sampled area at large scales. Naturally, there is a gradual transition between the SAR characterized by low  $z$ , which is typical for spatial scales smaller than typical range size (in which therefore the internal structure of species range plays the main role<sup>13,34</sup>), to the large-scale SAR, in which many species occur

only in a limited area, so that every increase of area leads to the addition of a substantial number of new species, with consequently high  $z$ . Although this general reasoning implies that the local slope (the derivative) of the SAR should be related to sizes of underlying geographic ranges, we are not aware of an existing demonstration that this is truly the case, and that mean range size is indeed the crucial factor which affects the overall shape of the SAR.

The formal approaches to upward-accelerating SAR at large scales have always been dependent on a particular set of assumptions, which have limited their general applicability. The model of ref. 2 assumes a random placement of species ranges which have constant (circular) shape within unlimited area. This simplified situation is analytically tractable, and the authors provide an equation which leads to upward-accelerating SAR with a local slope of  $z = 0.5$  for areas equal to mean species geographic range size. The authors contend that the SAR shape is given by the distribution of range sizes, so that a particular SAR shape is determined only by the mean and variance of this distribution. The limitation of this approach lies in its assumption concerning unlimited area. In reality, every studied area is limited, which leads to finite area effects in which the position of individual ranges within the studied domain necessarily affects the overall SAR shape<sup>34</sup>. The reason is that species ranges located more centrally are necessarily sampled by any large sampling window, as it is impossible to place the sampling window in such a way that it would not overlap given species range. On the other hand, species ranges which are located on the periphery of studied area are sampled only occasionally. This leads to higher species richness for large sampling areas if species ranges have the tendency to be located more centrally, in comparison to the situation where they are preferentially located on the periphery of the study area. This effect of nonrandom (more central) position of ranges occurs even if we place the ranges of constant shape randomly within the boundaries of given domain. If we assume a constant range shape (e.g. circles), large ranges always reach the central areas of the study plot, creating a mid-domain effect. Large sampling areas thus necessarily overlay these ranges, artificially increasing species richness at large scales if mean range sizes are relatively large in comparison to the size of the domain.

The SAR predicted by the neutral theory of biodiversity and biogeography<sup>4,5</sup> is also triphasic. Its shape is modulated by dispersal kernels and speciation rate, so that the area at which the third (upward-accelerating) phase emerges increases with the dispersal distance, and is proportional to the inverse of speciation rate<sup>5</sup>. This can be intuitively understood, as both dispersal distance and speciation rate are linked to the range size. Higher speciation

rates lead to rapid emergence of new, spatially restricted species, and thus increase species spatial turnover, especially if species have limited chance to spread over long distances. Distant sites are then more dissimilar to each other, and species number thus increases rapidly with area. In other words, higher speciation rate combined with low dispersal distances lead to higher proportion of species with smaller ranges, as many species are new and did not make it to spread out from their site of origin. Therefore, there is again a connection between range size and the SAR, although the general approach is constrained by particular assumptions of the neutral theory, namely demographic equivalence of all species.

To avoid the limitations of the formal approaches mentioned above, we have explored quantitative properties of the expected SAR under various scenarios. As in refs. 2 and 29, we assumed random placement of contiguous species ranges (contiguous ranges best correspond with the data we have used for the empirical SAR construction), but in some of the scenarios we attempted to avoid the mid-domain effect mentioned above.

### **D3 SARs and EARs resulting from the continent shape design**

The SARs and EARs constructed using the CS design are similar to those constructed using SNQ, although individual curves are less smooth (Supplementary Fig. 6), which is apparently due to the fact that small sample areas do not necessarily cover entire large areas. This incomplete sampling coverage affects the resulting SARs especially when areas of high species richness are located either (i) in peripheral regions of the continents (which are thus not reached by smaller areas of given shape, leading to lower species richness of smaller sample areas) or, conversely, (ii) in the centres of continents, which leads to an overestimation of species richness for smaller sample areas (because these repeatedly sample just the central hotspots). Consequently, the derivatives (local slopes) of these SARs and EARs vary widely (Supplementary Fig. 6d,h). However, the rescaled SARs still collapse into one general relationship very well (Fig. 2), indicating that there is indeed a general SAR for this continental scale that does not overly depend on sampling design.

### **D4 Interpretation of simulation model results**

Results for Models 1-4 are shown in Fig. 3 (for range-size distributions in the SNQ black areas in Supplementary Fig. 3) and in Supplementary Fig. 12 (for range size-distributions in the CS black areas in Supplementary Fig. 3). We find that the empirical SARs and EARs are very well approximated by a random placement of ranges with varying shape (Model 3). Importantly, both models of random range placement with varying range shapes (models 3

and 4) lead to almost perfect collapse of all the SARs into one universal curve. This is intriguing, considering that in these two models individual SARs were modeled using different range size frequency distributions. In contrast, Models 1 and 2 which introduced some artificial mutual dependence of species ranges, either by nonrandom placement of all ranges (Model 2) or by producing the mid-domain effect (leading to higher representation of species with large ranges in the central areas of the domain; Model 1), both distort the rescaled SARs and EARs, so that they are very different from the empirical ones. These results suggest that a universal curve emerges if the location of species ranges is random, i.e. if individual ranges are mutually independent to each other.

#### **D5 Spatial independence of empirical and modeled range locations and sizes**

The maps of centroids of observed geographic ranges (Supplementary Figs. 13-15) show distinct areas of higher centroid density, which corresponds to high spatial autocorrelation of centroid density at distances up to ~1,000-2000 km (Supplementary Figs. 13-15). Although this autocorrelation is in many cases higher than predicted by the random placement simulation models (in Eurasian, African and North-American data), in some cases the random placement model with mid-domain effect (Model 1) is capable of reproducing similar level of autocorrelation (especially in birds and mammals; Supplementary Figs. 13-15). At larger distances, centroid density of species' empirical ranges shows autocorrelation which is indiscernible from the random placement models and clearly different from the clumped Model 2 (Supplementary Figs. 13-15). The patterns are similar for the autocorrelation of the sizes of species' ranges (Supplementary Figs. 13-15, right columns). Even though empirical autocorrelation patterns concerning range sizes do mostly (but not always) deviate from the random placement models, they are much closer to the random placement models than to the highly clumped patterns produced by Model 2, which led to very poor collapse of SARs and EARs.

#### **D6 Causes of the deviations from the universal relationship**

Empirical SARs and EARs do deviate slightly from the universal curve predicted by the simulations, particularly at smaller spatial scales. This deviation can be attributed to the magnitude of spatial dependence (aggregation) in the position of individual ranges. We have shown that the distribution of empirical ranges is often slightly more clumped than that expected from the random placement models (see above), but that the observed aggregation is much lower than in the case of Model 2, which led to very poor collapse of SARs and

EARs. Notably, the character of the deviations of the EAR curves in the CS design (Fig. 3) is somewhat similar to the deviations produced by Model 2 (Supplementary Fig. 12), although the EAR deviations in the empirical dataset are not as strong. This is expected, given that the magnitude of empirical range aggregation is much weaker than in Model 2, as described above.

We suggest that the deviations of the empirical SARs and EARs from the universal curves can also be attributed to the much greater complexity of empirical compared to modeled range shapes. In contrast to simple geometrical objects such as rectangles (simulated ranges) they exhibit porosity (fragmentation, gaps) and more complex shapes. Consequently, for the same number of occupied grid cells empirical ranges will often reach more distant areas than would be the case if they were fully contiguous. Thus, empirical species richness measured at large scales (i.e. using large sampling windows) will be higher, since many species will occur in large areas even if the number of occupied grid cells is relatively low. This will lead to a steeper SAR than predicted by the simulation model. Indeed, several observed SARs reveal slightly lower species richness at small scales than predicted. Note that all the curves are standardized so that the species richness for the area corresponding to mean range size is the same. Therefore, the steeper SARs must reveal relatively lower richness at scales smaller than the scale of mean range size.

## Supplementary Tables

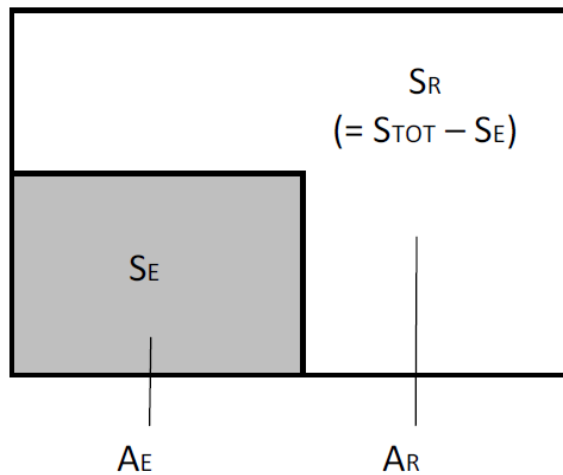
**Supplementary Table 1 | Summary of the species distribution data.** We used the same expert information for species geographic ranges as described in ref. 18. We excluded non-breeding ranges for birds and limited our analyses to the five major continental landmasses. The geographic range data for birds has recently been validated to be reliable down to ca. 100-150km resolution<sup>19</sup>, and we thus chose 110 km × 110 km as finest plot size accurately representing presence and absence for all taxa. SNQ refers to the strictly nested design; CS refers to the continental design.

Taxon	Continent	SNQ			CS		
		# of species	# of records	Mean range size [# of grid cells]	# of species	# of records	Mean range size [# of grid cells]
Birds	Eurasia	1495	423,897	283.5	1866	730,322	391.4
	Africa	1820	464,159	255.03	1887	540,543	286.45
	N. America	657	131,414	200.02	1541	288,196	187.02
	S. America	2760	522,791	189.42	3003	625,195	208.19
	Australia	527	66,787	126.73	597	106,457	178.3
	All continents	6285	1,609,048	221.66	7652	2,290,713	257.56
Mammals	Eurasia	869	143,296	164.9	1149	245,355	213.54
	Africa	1052	174,107	165.5	1136	199,548	175.66
	N. America	388	53,954	139.06	812	110,700	136.33
	S. America	1075	173,062	160.99	1201	205,936	171.47
	Australia	228	15,891	69.7	274	25,270	92.23
	All continents	3267	560,310	155.12	4177	786,809	172.09
Amphibians	Eurasia	459	17,162	37.39	794	35,183	44.31
	Africa	635	42,619	67.12	712	47,731	67.04
	N. America	219	10,087	46.06	906	24,751	27.31
	S. America	1641	72,529	44.2	2030	81,802	40.15
	Australia	151	5,147	34.09	213	9,001	42.26
	All continents	2947	147,544	47.51	4530	198,168	42.57
All taxa	All continents	12499	2,316,902	165.78	16359	3,275,690	42.57

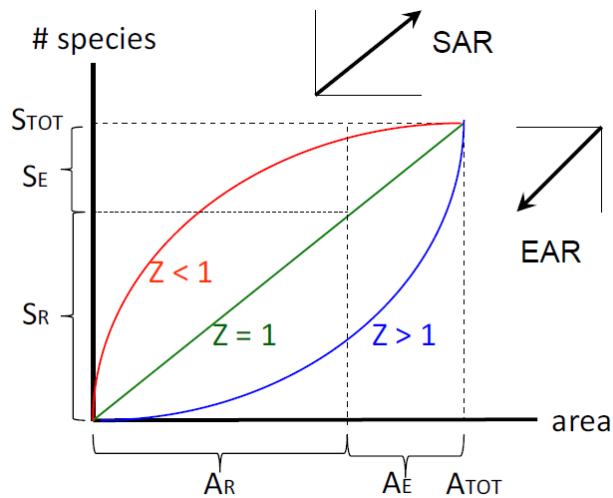
**Supplementary Table 2 | Slopes of the EARs and SARs calculated using the continent shape (CS) design.** The slopes were estimated by using linear regression on logarithms of the mean number of species at each of the areas (which were logarithmically transformed as well). The EAR slopes were calculated for the same range of areas that were used in the SNQ design ( $\log_{10}$  Area  $\leq 6.7$ ), the SAR slopes were calculated for the areas that have  $\leq 100$  grid cells ( $\log_{10}$  Area  $\leq 6.1$ ; the left part of the SAR plots in Supplementary Fig. 4) and areas that have  $\geq 250$  grid cells ( $\log_{10}$  Area  $\geq 6.48$ ; the right part), providing measures concerning both lower and upper end of the upward-accelerating SARs. To give an idea about the possible range of slopes that can be detected when incomplete biodiversity data are available we randomly selected only 10% of the original data, repeated the procedure 500 times and estimated the lower and upper 95% quantiles of the slopes obtained from the re-sampled data.

Continent	Taxon	EAR slope	SAR slope	SAR slope
		( $\log_{10}$ Area $\leq 6.7$ )	( $\log_{10}$ Area $\leq 6.1$ )	( $\log_{10}$ Area $\geq 6.48$ )
Birds	Africa	1.26 (1.03-1.65)	0.2 (0.18-0.23)	0.34 (0.28-0.37)
	Australia	1.22 (0.8-2.09)	0.13 (0.1-0.15)	0.48 (-0.51-1.59)
	S. America	1.24 (1.01-1.43)	0.19 (0.17-0.21)	0.47 (0.31-0.47)
	N. America	0.68 (0.34-1.43)	0.17 (0.15-0.19)	0.74 (0.09-0.75)
	Eurasia	1.02 (0.65-2.02)	0.18 (0.16-0.19)	0.5 (0.46-0.56)
Mammals	Africa	1.19 (1-1.48)	0.22 (0.2-0.25)	0.47 (0.4-0.51)
	Australia	1.23 (1.03-1.48)	0.19 (0.16-0.21)	0.79 (-1.02-2.27)
	S. America	1.18 (1.04-1.37)	0.19 (0.17-0.21)	0.54 (0.45-0.55)
	N. America	0.6 (0.31-0.91)	0.19 (0.16-0.21)	0.81 (0.24-0.86)
	Eurasia	1.16 (0.9-1.45)	0.22 (0.2-0.23)	0.6 (0.51-0.62)
Amphibians	Africa	1.13 (1.02-1.29)	0.28 (0.24-0.32)	0.67 (0.52-0.73)
	Australia	0.85 (0.65-1.02)	0.23 (0.18-0.27)	1.22 (-1.63-1.68)
	S. America	0.9 (0.82-1.02)	0.29 (0.26-0.32)	1.02 (0.57-0.99)
	N. America	0.5 (0.33-0.75)	0.26 (0.22-0.31)	1.57 (-2.27-1.73)
	Eurasia	0.97 (0.78-1.22)	0.28 (0.23-0.33)	1.14 (0.7-1.18)

## Supplementary Figures and Legends



**Supplementary Figure 1 | Simple graphical representation of the key terms in the relationship between SAR and EAR.** The total area of the studied region,  $A_{TOT}$ , comprises the area within which the number of endemic species,  $S_E$ , is sampled, and the remaining area  $A_R$ , for which we assume some particular species-area relationship, i.e. that number of species  $S_R$  is predictably related to  $A_R$ . Since endemic species by definition do not occur outside  $A_E$ , the number of species which occur in the remaining area,  $S_R$ , is equal to the difference between  $S_{TOT}$  and  $S_E$  (and consequently,  $S_E = S_{TOT} - S_R$ ).



**Supplementary Figure 2 | Graphical representation of the relationships between the EAR and the SAR.** If the SAR for species richness in non-sampled (remaining) area  $A_R$  can be represented as a power-law, then it is a downward-decelerating (concave) curve if  $z < 1$  (upper red curve) and upward-accelerating (convex) curve if  $z > 1$  (bottom blue curve). If  $z = 1$ , then it is represented by a line (green), and in such a case the relationship between the number of endemic species,  $S_E$ , and  $A_E$ , is also linear, corresponding to a power-law with  $z = 1$  (this situation corresponds to  $S_E$  and  $S_R$  on the vertical axis of the plot). The reason is that the EAR can be read as an increase of endemic species number with area by beginning by top right corner, and moving left and down, since  $A_E = A_{TOT} - A_R$  and  $S_E = S_{TOT} - S_R$ .

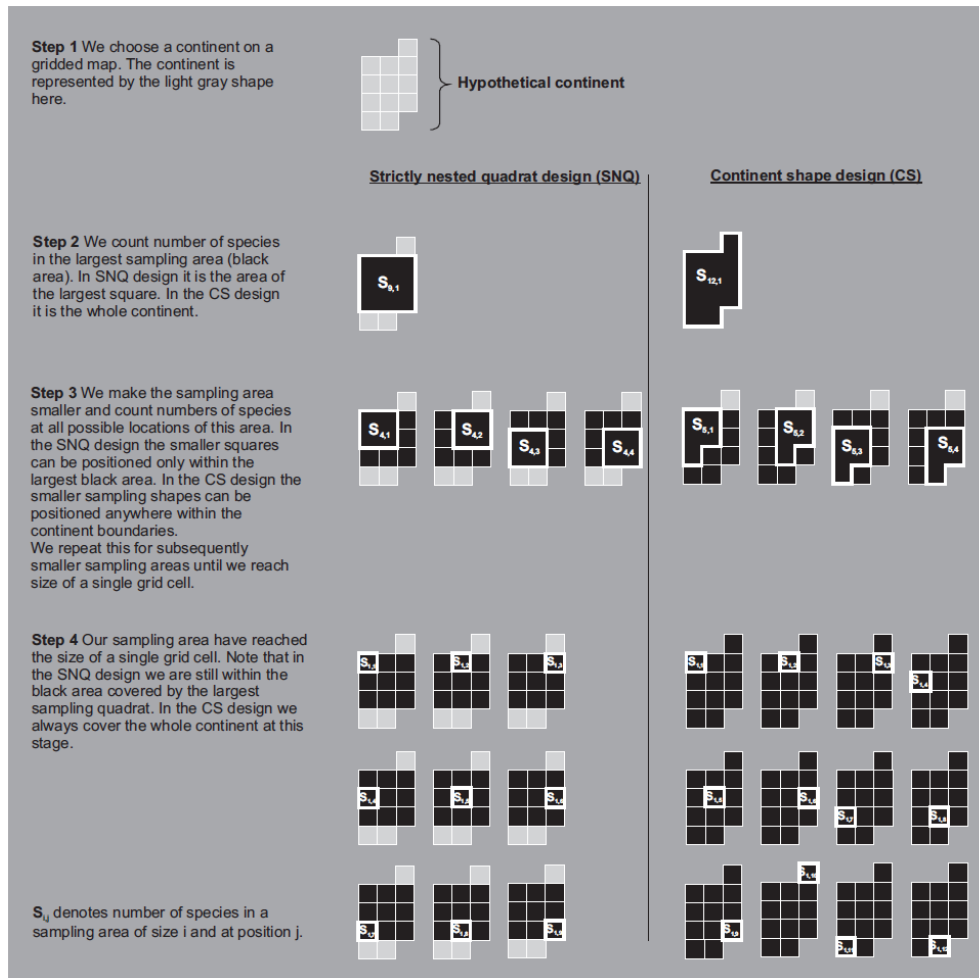
## Strictly Nested Quadrat (SNQ) design



## Continent Shape (CS) design



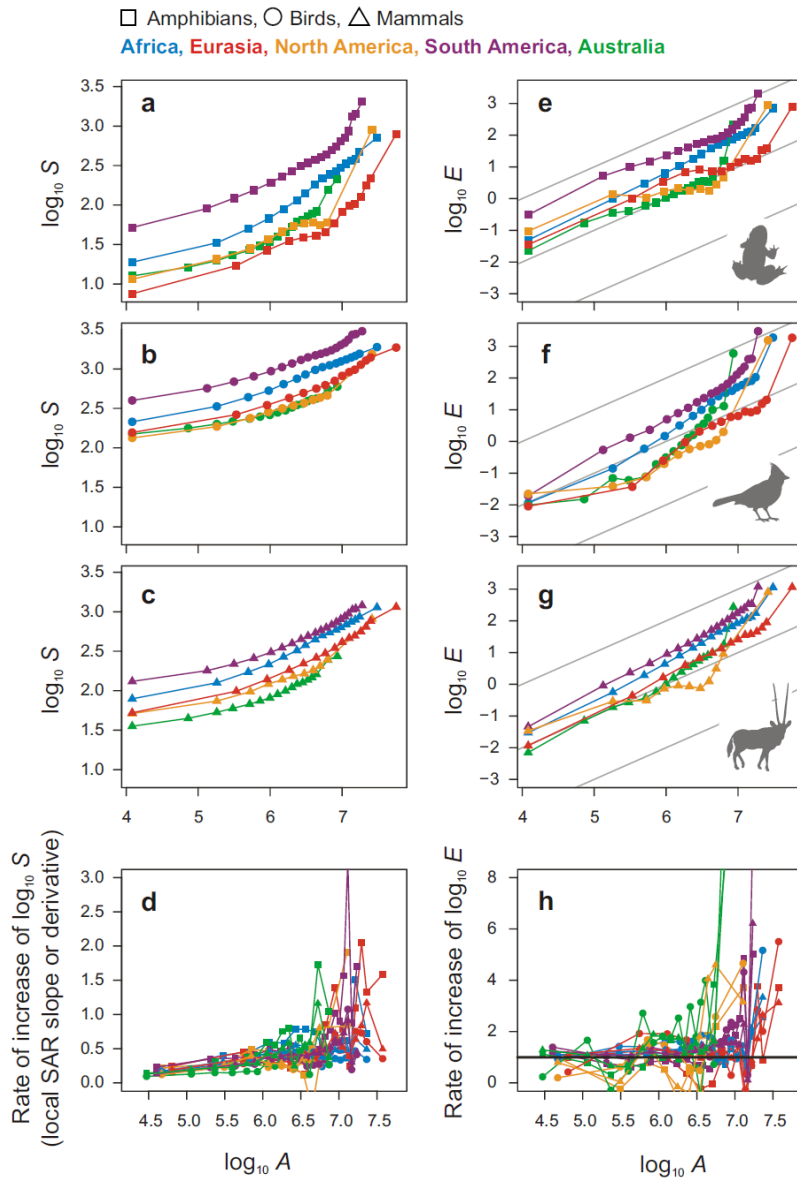
**Supplementary Figure 3 | Geographic coverage of the SNQ and CS designs used in our study.** In the case of SNQ, the largest size of the sampling windows used for four largest continents was 20×20 grid cells. However, we could not fit this window to Australia and we used the size of 14×14 instead.



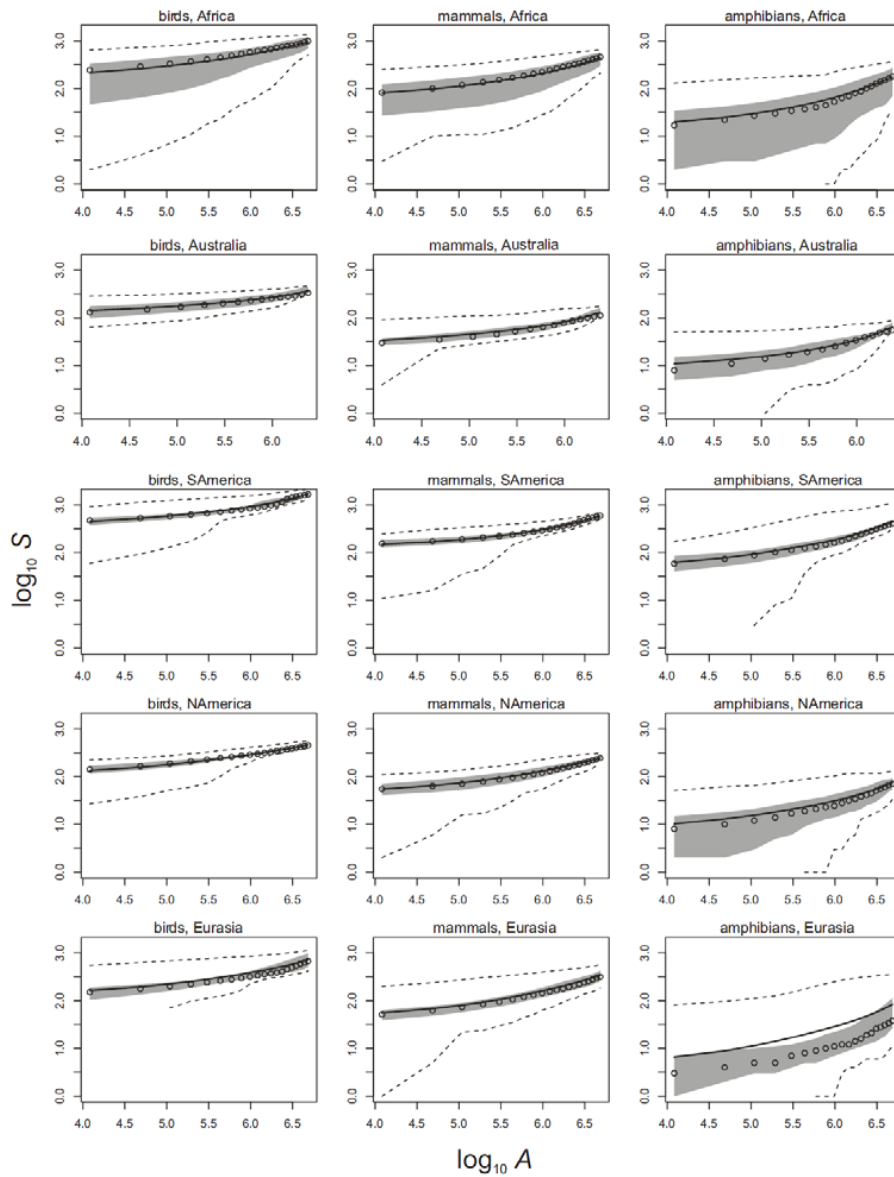
**Supplementary Figure 4 | Illustration of the sampling designs used.** The strictly nested quadrat design is unable to cover the whole area of a continent, as peripheral regions cannot be covered by large rectangular sample areas, and thus they are excluded. In the continental shape design, which is based on resizing the original sample area of the whole continent, smaller sample plots do not sample exactly the same region as large plots, as smaller shapes fit inside larger (irregular) plots only in particular locations.



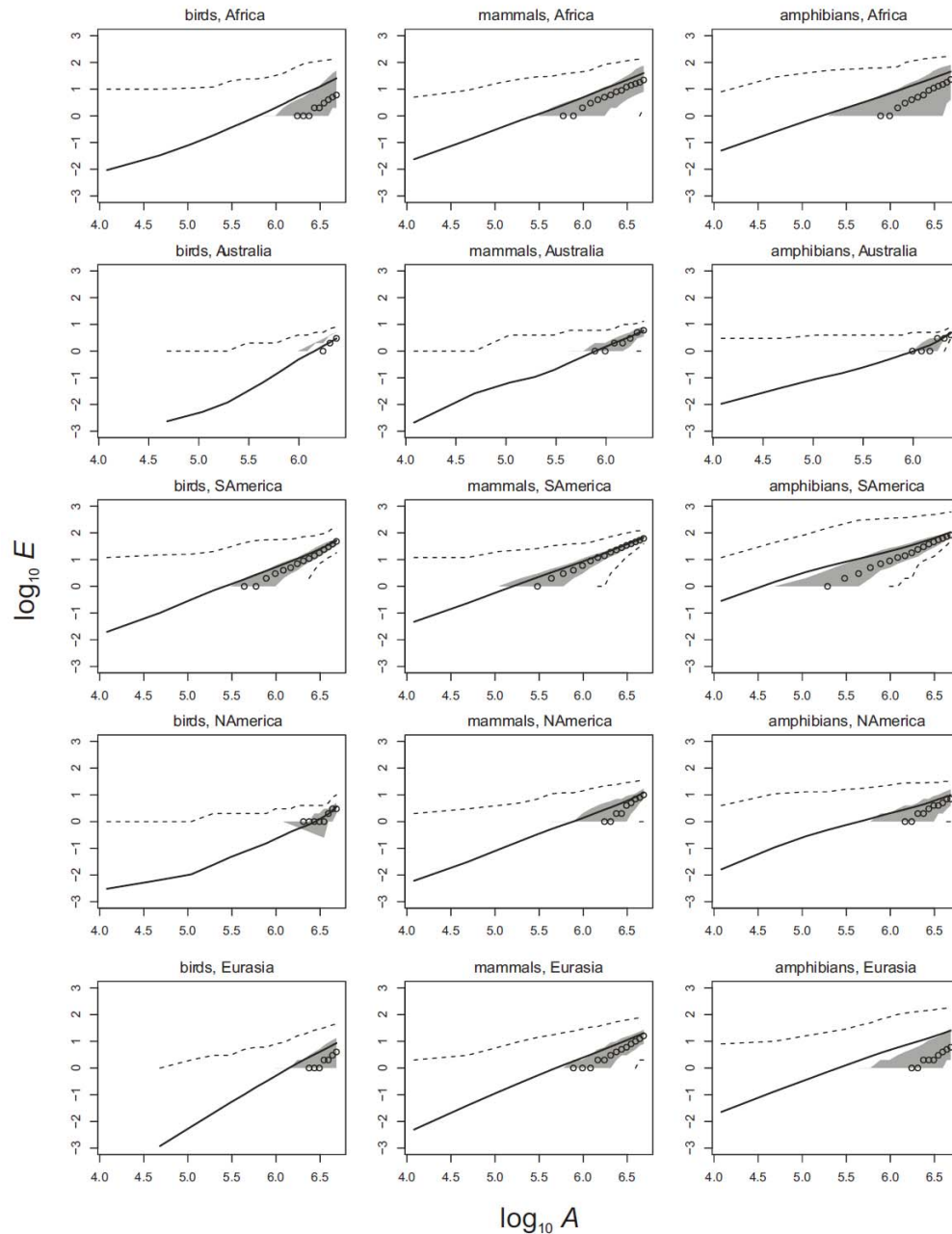
**Supplementary Figure 5 | Illustration of the continent shape (CS) design.** Here coordinates of the Africa's grid cells were multiplied by  $k = 0.3$  in order to get the smaller Africa shape, which was then moved around Africa as a sampling window. The smaller sampling plots can overlap each other, but still they cannot fully cover the whole shape of the larger plots. This may lead to underrepresentation of some areas and consequent scatter in the data (Supplementary Fig. 4).



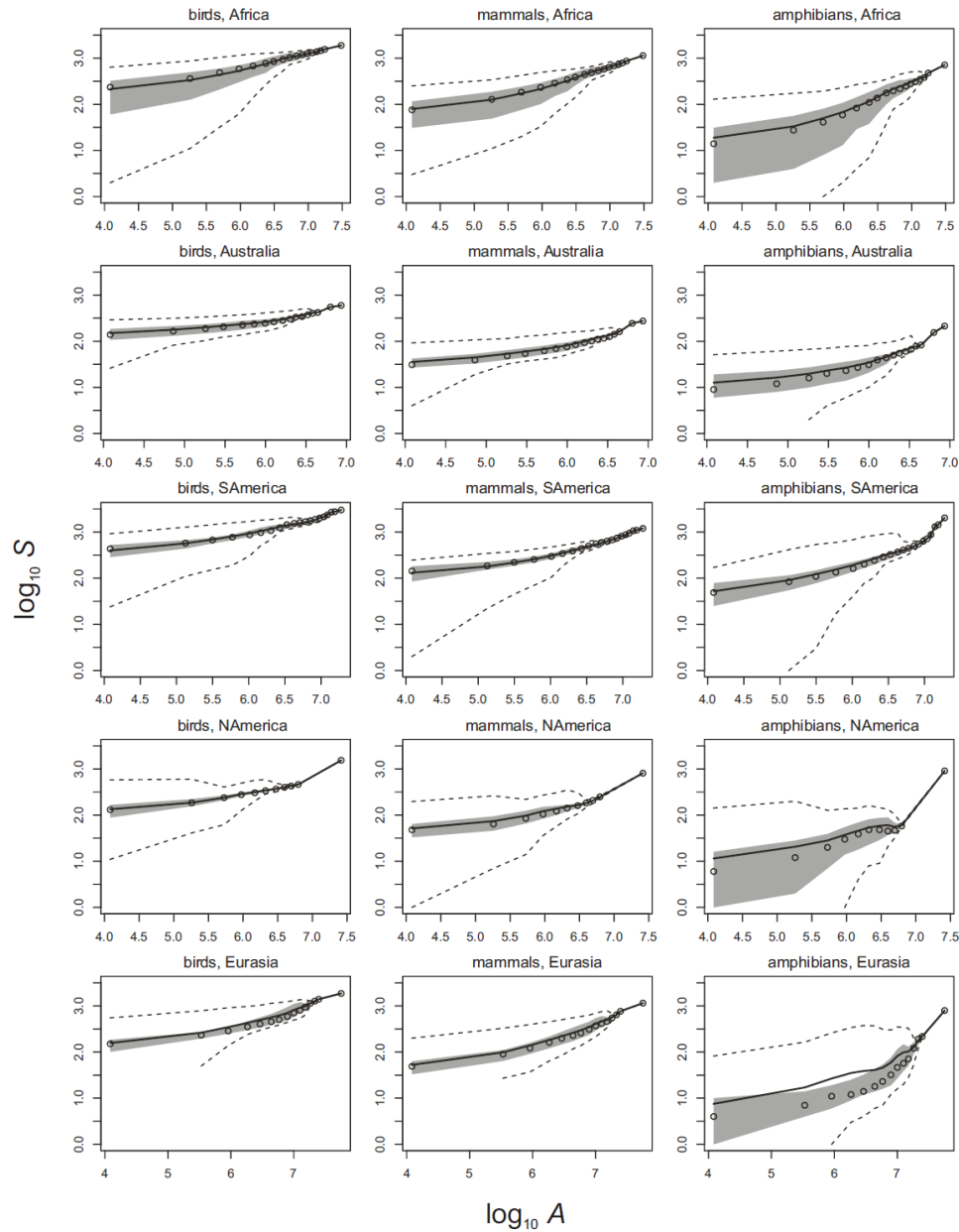
**Supplementary Figure 6 | Species-area and species-endemics relationships (SARs and EARs) for four continents and three major taxa calculated using the continent shape (CS) design.** See Fig. 1 for comparison with the SNQ design.  $S$  is mean number of species,  $E$  is mean number of endemics,  $A$  is area [ $\text{km}^2$ ], grey lines correspond to a power-law with slope 1, i.e. the proportionality between area and the number of species. Note that the local slopes for particular areas (d, h) vary considerably due to sampling issues (see above).



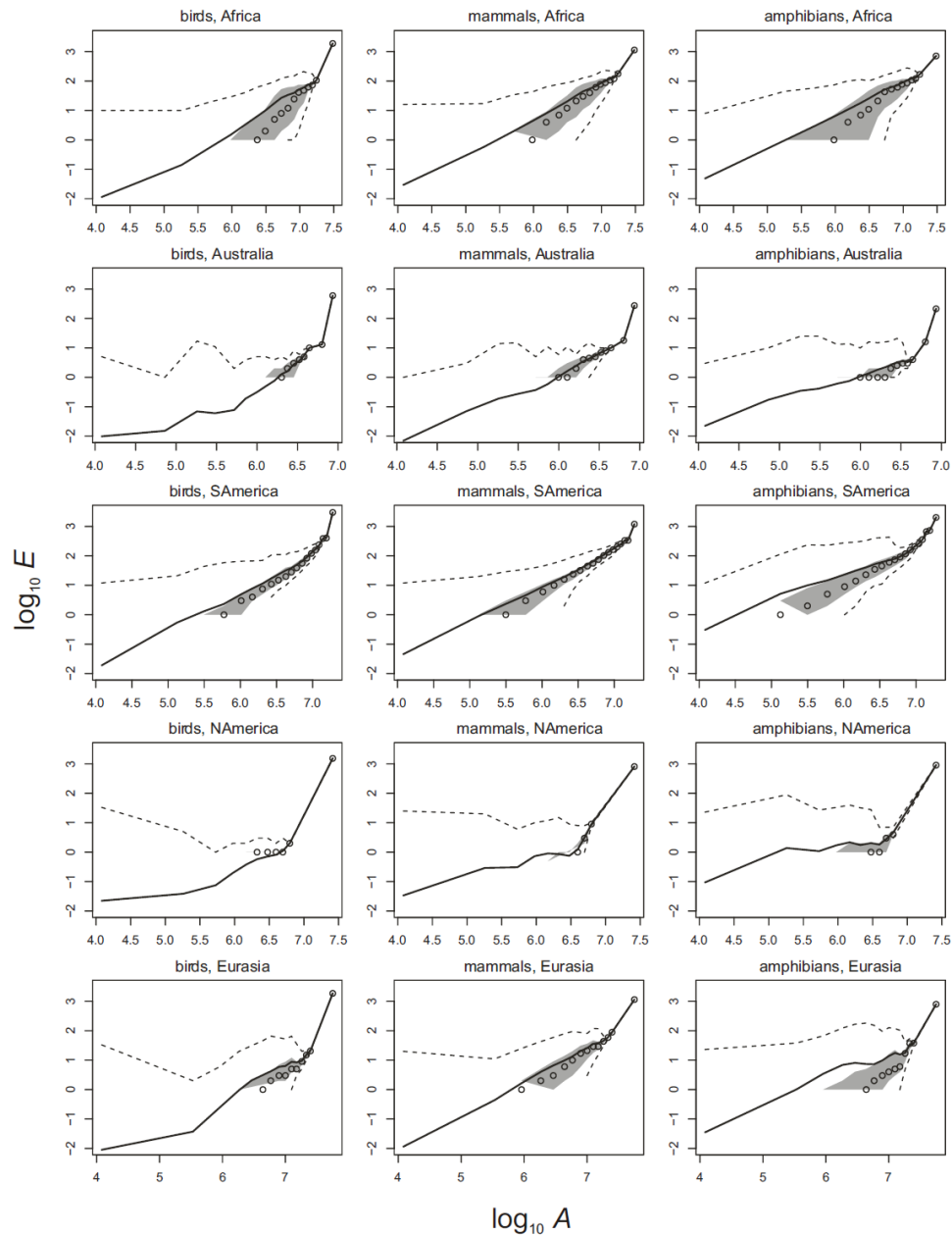
**Supplementary Figure 7 | Plots showing detailed structure of the SARs based on strictly nested quadrat (SNQ) design.** Solid lines are  $\log_{10}$  of mean values of number of species. Open circles are  $\log_{10}$  of medians of number of species. Dashed lines are  $\log_{10}$  of minimum and maximum values of number of species. Grey areas delineate  $\log_{10}$  of 25% and 75% quantiles of number of species. No values are plotted in case that there were zero values of number of species (because  $\log_{10}$  of 0 is not defined).



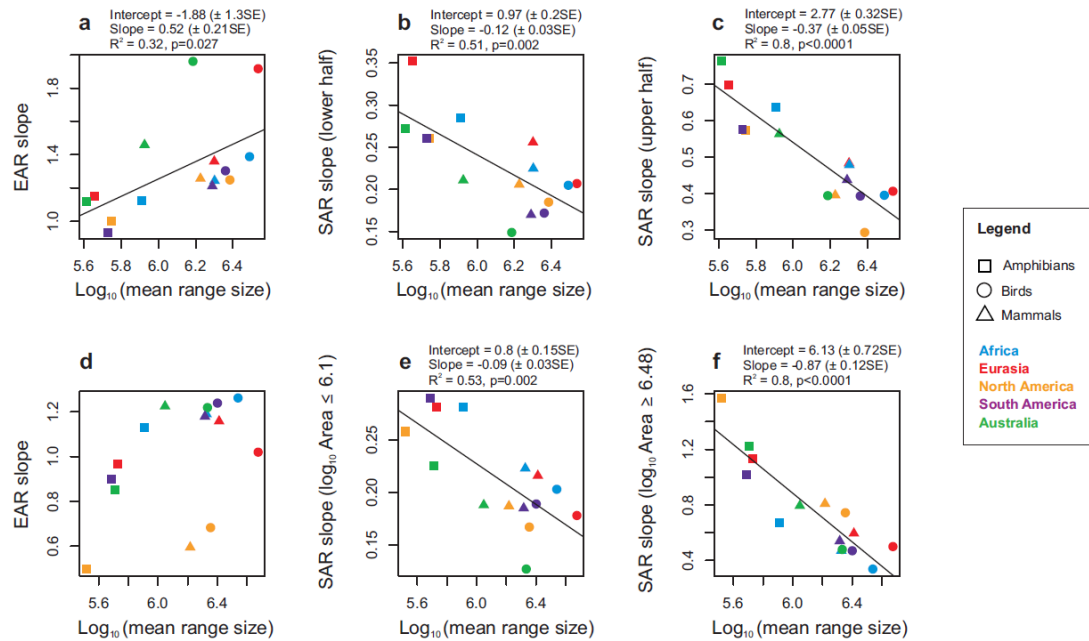
**Supplementary Figure 8 | Plots showing detailed structure of the EARs based on strictly nested quadrat (SNQ) design.** Solid lines are  $\log_{10}$  of mean values of number of endemic species. Open circles are  $\log_{10}$  of medians of number of endemic species. Dashed lines are  $\log_{10}$  of minimum and maximum values of number of endemic species. Grey areas delineate  $\log_{10}$  of 25% and 75% quantiles of number of endemic species. No values are plotted in case that there were zero values of number of species (because  $\log_{10}$  of 0 is not defined).



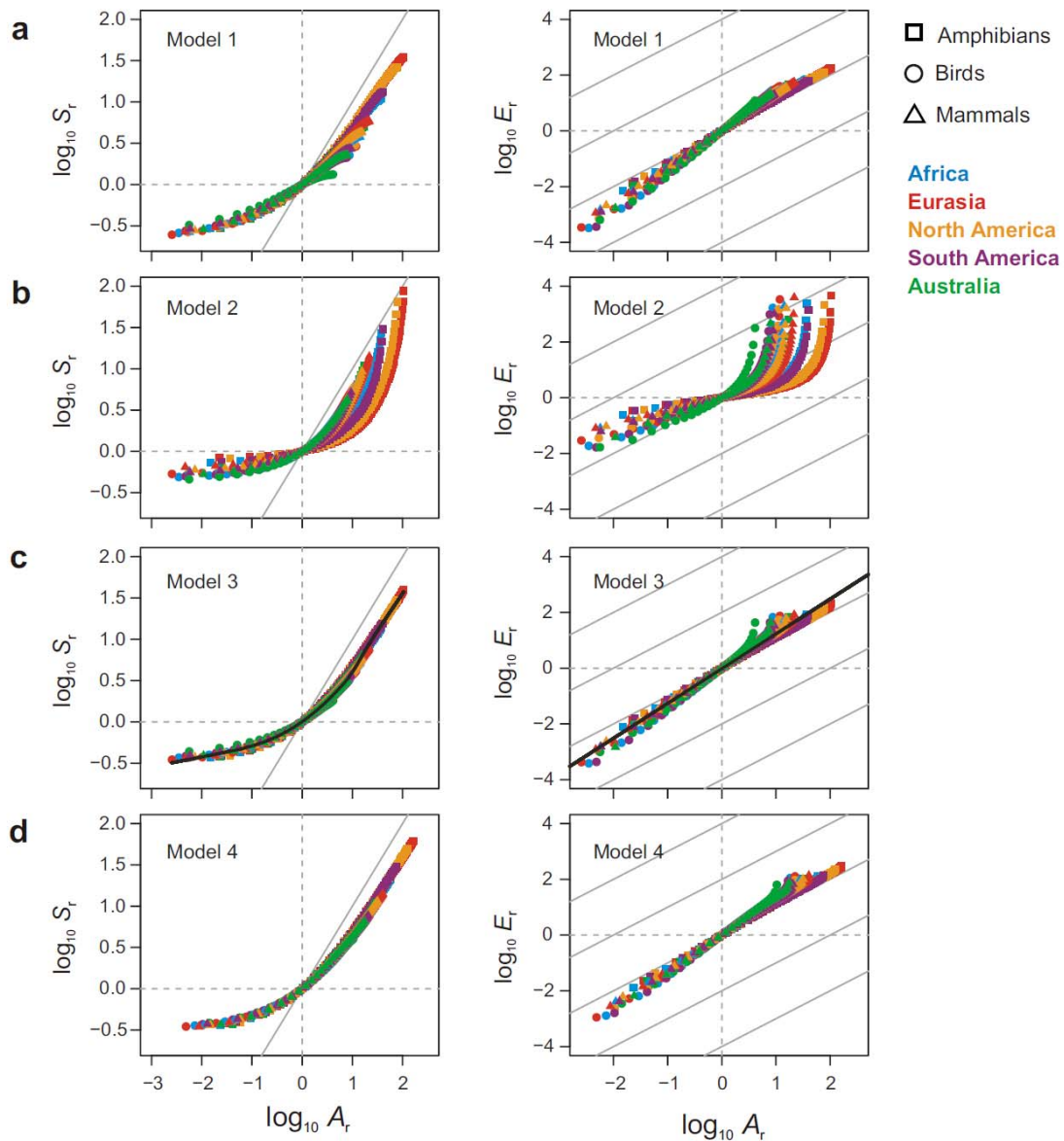
**Supplementary Figure 9 | Plots showing detailed structure of the SARs based on continent shape (CS) design.** Solid lines are  $\log_{10}$  of mean values of number of species. Open circles are  $\log_{10}$  of medians of number of species. Dashed lines are  $\log_{10}$  of minimum and maximum values of number of species. Grey areas delineate  $\log_{10}$  of 25% and 75% quantiles of number of species. No values are plotted in case that there were zero values of number of species (because  $\log_{10}$  of 0 is not defined).



**Supplementary Figure 10 | Plots showing detailed structure of the EARs based on continent shape (CS) design.** Solid lines are  $\log_{10}$  of mean values of number of endemic species. Open circles are  $\log_{10}$  of medians of number of endemic species. Dashed lines are  $\log_{10}$  of minimum and maximum values of number of endemic species. Grey areas delineate  $\log_{10}$  of 25% and 75% quantiles of number of endemic species. No values are plotted in case that there were zero values of number of species (because  $\log_{10}$  of 0 is not defined).

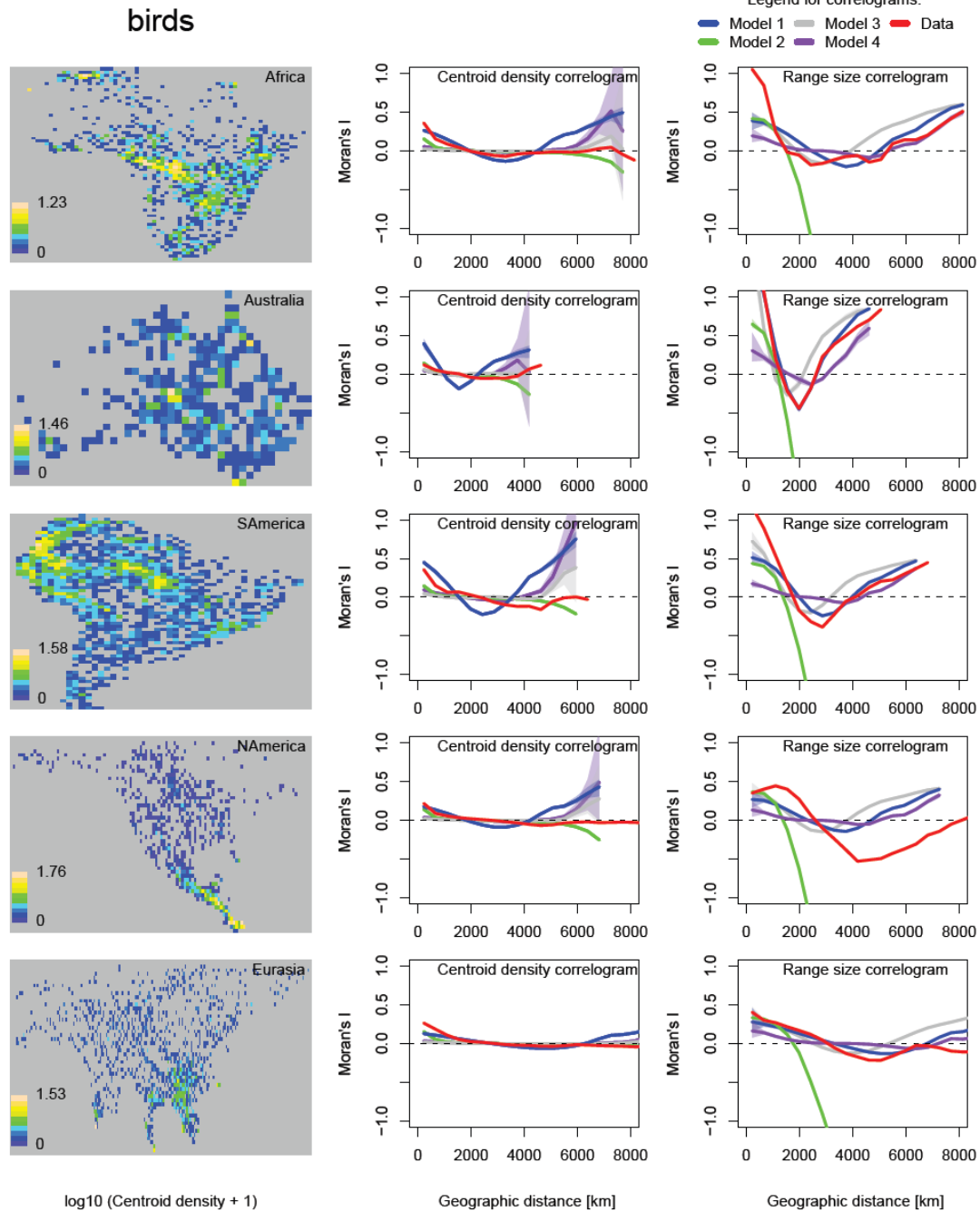


**Supplementary Figure 11 | Relationships between mean range size and the slopes of SARs and EARs.** a, b and c refer to the strictly nested quadrat design; d, e and f refer to the continent shape design. In a, d, e and f the mean range size refers to the range size within the whole continent whereas in b and c the range size was taken only from the area covered by the SNQ sampling design. For more details and exact slope values see Table 1 and Supplementary Table 2.



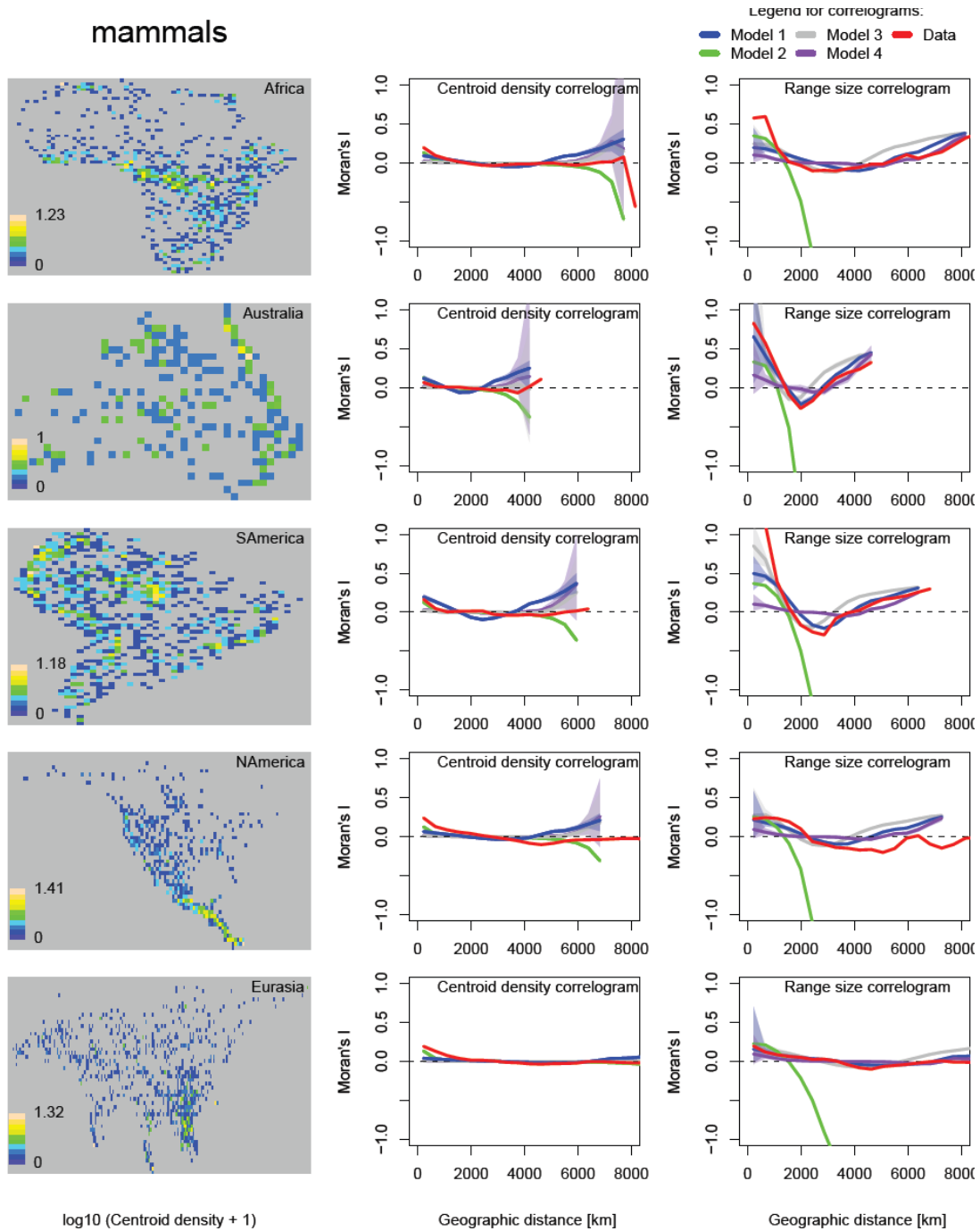
**Supplementary Figure 12 | The rescaled SARs and EARs predicted by four simulation models of range placement (for domain size and range-size frequency distribution of the CS design).**

Range sizes were drawn from empirical frequency distributions of each taxon and domain (black areas in Supplementary Fig. 3) and were placed into a domain with size equal to that of the original SARs and EARs constructed using the continent shape design (Supplementary Fig. 3). We produce a fitted line for Model 3 results to highlight its match with the empirical patterns (see Fig 2): black lines represent the lowess regression line for the rescaled SAR plot (smoothing span 0.2) and the linear regression line for the rescaled EAR plot. Solid grey lines all have a slope of one.

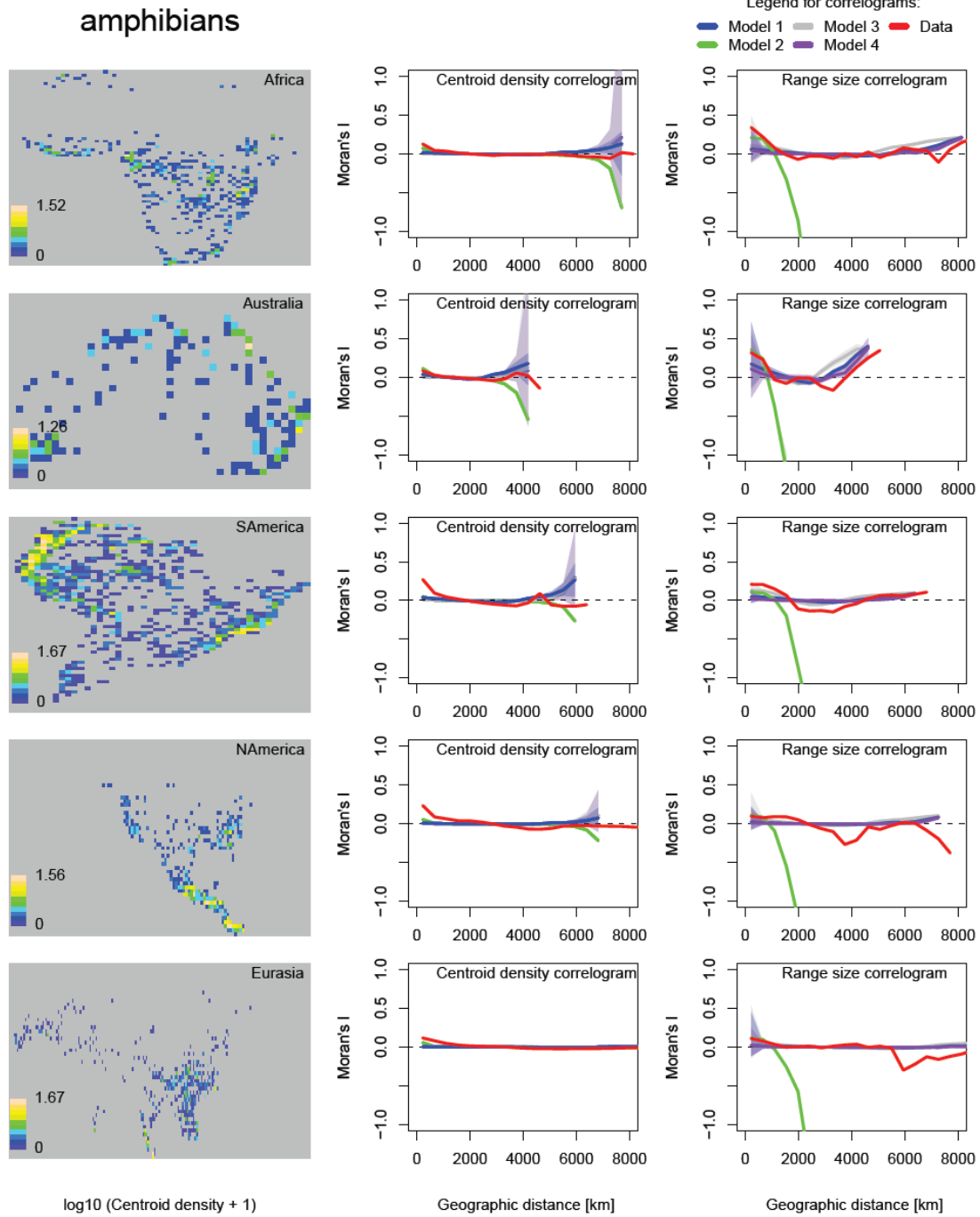


**Supplementary Figure 13 | Spatial distribution and autocorrelation of centroids and sizes of geographic ranges of birds.** The analysis compares the empirical patterns with those produced by simulation models 1-4. The maps show density of range centroids ( $\log_{10}(x+1)$  transformed) in each grid cell. Centroids that lie outside of mainland areas are not mapped. Centroid density correlograms were calculated using only the mainland centroids. Range size correlograms were calculated using all ranges (even those with centroids that lie in the sea). Filled polygons in the correlograms are 95% confidence intervals of the models. Continent delineation is identical to that used in the CS design.

mammals



**Supplementary Figure 14 | Spatial distribution and autocorrelation of centroids and sizes of geographic ranges of mammals.** For other details see Supplementary Fig 13.



**Supplementary Figure 15 | Spatial distribution and autocorrelation of centroids and sizes of geographic ranges of amphibians.** For other details see Supplementary Fig 13.